Suspended slab and photonic crystal waveguides in lithium niobate

Guangyuan Si
Department of Electrical and Computer Engineering, Centre for Optoelectronics, National University of Singapore, 4 Engineering Drive 3, Singapore 117576, Singapore

Ee Jin Teo and Andrew A. Bettiol
Department of Physics, Centre for Ion Beam Applications, National University of Singapore, 2 Science Drive 3, Singapore 117542, Singapore

Jinghua Teng
Institute of Materials Research and Engineering, 3 Research Link, Singapore 117602, Singapore

Aaron J. Danner[a)]
Department of Electrical and Computer Engineering, Centre for Optoelectronics, National University of Singapore, 4 Engineering Drive 3, Singapore 117576, Singapore

(Received 2 November 2009; accepted 25 January 2010; published 22 March 2010)

Suspended waveguides have been widely applied to silicon-on-insulator structures because they are easily fabricated with processing techniques similar to those of integrated circuit design. However, it is difficult to fabricate such structures in lithium niobate, which is also a very important material for optoelectronics. One main challenge is the difficulty of etching lithium niobate. In this work, the authors show a method to fabricate suspended slab waveguides in lithium niobate by combining ion implantation, focused ion beam milling, and selective wet etching techniques. The method does not involve wafer bonding or crystal ion slicing and is entirely monolithic. Lattice damage can be introduced to a buried thin layer of a certain depth beneath the sample surface by ion implantation, resulting in a considerable wet etching selectivity to bulk material. The etching rate has been investigated to control the size of the suspended membrane. Fabrication of suspended photonic crystal waveguides has also been demonstrated. The results show an effective method of fabricating suspended devices in lithium niobate, which enables new applications such as waveguides, modulators, and infrared detectors. [DOI: 10.1116/1.3327925]

I. INTRODUCTION

Lithium niobate [$LiNbO_3$ (LN)] has drawn much attention because of its peculiar optical properties such as acousto-optic, electro-optic, piezoelectric, and ferroelectric effects. Conventionally, a waveguide in a LN crystal is fabricated with metal diffusion, ion exchange, or proton exchange techniques. Waveguides in LN are used for high-speed modulation or for nonlinear devices such as parametric oscillators and amplifiers. LN is also common in telecommunications systems due to its high electro-optic coefficient and low optical losses. Moreover, LN is an important ferroelectric material, which is extensively used in optoelectronic and surface acoustic wave devices. In addition, the fabrication of LN photonic crystals (PCs) could find application in decreasing the size of crucial components in many optical systems. The fabrication of PC structures, however, requires high-index-contrast materials to create vertical and in-plane index confinement, which is impossible to achieve with diffusion or proton exchange methods. In particular, PC slab structures in LN would offer the possibility of realizing high-density integrated optical systems and low-loss large-bandwidth connectivity between different components in integrated circuits on an active material. The optical properties could then be modified externally through an applied electric field, for example, offering fast tunability of PC devices.[1–3] Because the Pockels effect in LN is much faster (and loss is lower) than carrier-induced index changes in silicon-on-insulator (SOI) structures, for example, our method could allow applications requiring ultrahigh switching speeds in LN that would be impossible to achieve in other materials.

Mature etching techniques are needed to produce smooth and vertical etching surfaces. However, it is very difficult to etch LN due to its poor reactivity with common etchants and selectivity issues. There are two common methods of etching LN: wet etching and plasma etching. Wet etching is a frequently used processing step but is seldom applied to LN because of the material's strong etch resistance, which results in low etch rates and nonuniform etching profiles.[4,5] For plasma etching, the main limitation is the redeposition of LiF, which will lower the etching rate when fluorine gases are involved in the process. To improve this, a mixture of fluorine gases and argon or oxygen has been proposed.[6,7]

Suspended membrane waveguides have ultralow loss and strong light confinement due to the large refractive index contrast. However, most slab-type waveguide designs with PCs are limited to SOI-based structures.[8–10] In such systems, light is confined in the silicon slab and is guided by a periodic array of holes etched through the slab. The buried oxide can be easily removed by a selective wet etch. By replacing the out-of-plane asymmetric structure (air-silicon-silicon dioxide) by a symmetric frame (air-silicon-air), the propaga-

[a)]Electronic mail: adanner@nus.edu.sg

tion loss can be reduced remarkably. Besides, it can provide high-density integration of optical components due to strong light confinement and tailorable dispersion. Similar methods can be applied to GaAs/AlAs systems by oxidizing AlAs and undercutting with a wet etch. No such methods are normally available in bulk LN. In this article, we report on the fabrication of suspended membrane and PC structures in LN. Our method can effectively be applied to bulk LN wafers, which are typically of much higher quality than epitaxial LN (which we do not investigate). We show effective wet etching of implanted LN after the formation of a buried sacrificial layer beneath the sample surface induced by ion damage. We also demonstrate large area PCs fabricated in the suspended membrane. Our approach opens a new era of LN-based device design.

II. FABRICATION

In the past, ion implantation techniques have been applied to LN together with a wafer bonding method to transfer a thin film of LN to another substrate such as silicon or gallium arsenide to make a slab waveguide.[11,12] X-ray probing can be applied to map elastic strains caused by implantation.[13] The refractive indices and the electro-optical coefficient of the fabricated thin films have also been studied elsewhere.[14,15] Recently, ultrathin membranes are available in x-cut LN (Ref. 16) and the PCs in an ion-sliced LN film with a soft underlayer have been characterized.[17] Devices fabricated using such a method have advantages over normal waveguides fabricated by etching proton exchanged or metal diffused LN because they not only have low loss and tight optical confinement but also enable the fabrication of PC structures. Our process is different: a buried sacrificial layer below the sample surface can be generated directly by ion implantation due to lattice damage, which results in a large etch selectivity relative to the bulk LN.

The schematic drawing showing the process flow is illustrated in Fig. 1. First, He^+ ions with 1 MeV beam energy were implanted normal to the surface of a z-cut LN sample. According to Stopping and Range of Ions in Matter (SRIM) (Ref. 18) simulation shown in Fig. 2(a), the damage is rather constant and low for the first 2 μm from the surface and increases sharply by 20 times at the end of range of 2.4 μm. This is also known as the Bragg peak. For a dose of 1×10^{16} ions/cm^2 used in this experiment, this corresponds to a damage of 4×10^{20} vacancies/cm^3 created near the surface and a maximum of 8×10^{21} vacancies/cm^3 created at the end of range. The lattice defects introduced by implantation make it chemically active toward selective etching compared to a perfect crystal. Figure 3 shows that selective etching occurs only near the end of range, producing a 2 μm thick LN slab that is suspended in air with a gap thickness of about 350 nm. To prevent light leakage into the substrate, a thicker air gap may be needed. This can be obtained by using multienergy irradiations to produce overlapping Bragg peaks to increase the etched layer thickness. In Fig. 2(b), we show that the thickness of the etched layer can be increased to 1 μm by using irradiations with three different energies (0.8, 1, and 1.15 MeV). After implantation, rectangular patterns were milled by focused ion beam (FIB) etching in the implanted area which also exposed the sacrificial layer to chemicals during wet etching. During FIB milling, gallium ions with 30 keV acceleration voltage were emitted and focused on the sample surface. The probe current was 350 pA and the spot size was about 55 nm. Finally, the sample was immersed in a mixture of 65% HNO_3 and 49% HF (2:1) for various times to etch away the damaged layer, leaving suspended structures consisting of a LN slab vertically surrounded by air. The process is simple and monolithic. Optical lithography or electron beam lithography, combined with inductively coupled plasma etching, can also be used to mill the pattern prior to wet etching the undercut region.

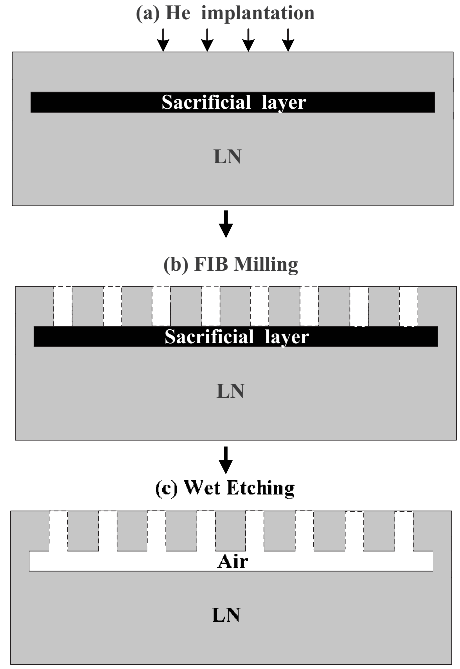

FIG. 1. Illustration of the process steps to create suspended structures in LN using ion implantation, FIB milling, and selective wet etching.

III. RESULTS AND DISCUSSION

The scanning electron microscope (SEM) image of a rectangular hole milled by FIB on the edge of the implanted area after wet etching is shown in Fig. 3. The picture was taken at a glancing incidence of 35° to normal. One can observe the undercut structure clearly which is caused by selective wet etching. The layer of the sacrificial LN replaced by air has a conical shape, indicating a selectivity of the sacrificial to the bulk. Images of a poststructure fabricated by ring FIB milling of 8 μm in diameter before and after wet etching are demonstrated in Figs. 4(a) and 4(b), respectively. Again, there is an undercut structure formed after wet etching. The undercut centers 2 μm below the sample surface. However, in Fig. 4(a), one can see that the surroundings of the milled ring are damaged because of a large probe current during milling. In addition, it is evident that the profiles are not vertical, which is common in FIB milling. Improving the

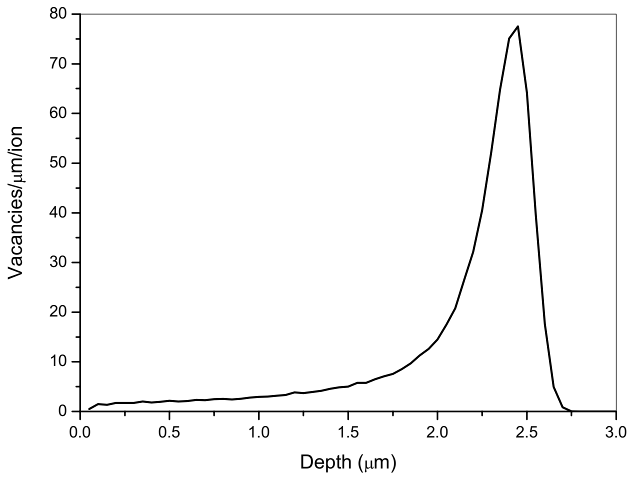

(a)

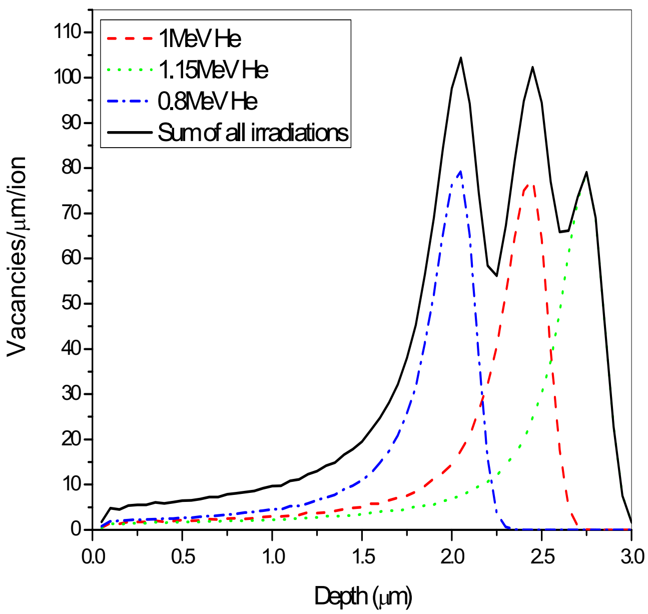

(b)

FIG. 2. (Color online) (a) SRIM simulation of 1 MeV He^+ in LN. (b) SRIM simulations of 0.8, 1, and 1.15 MeV He^+ in LN.

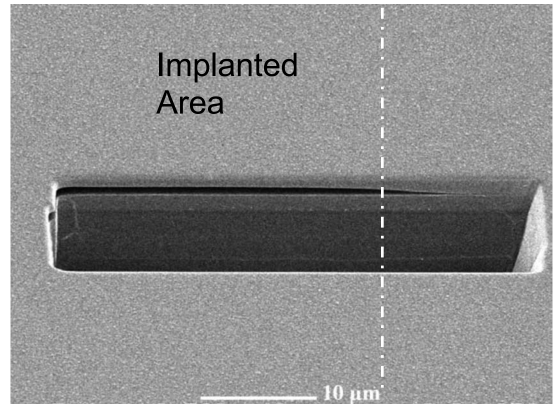

FIG. 3. SEM image of a rectangular hole patterned on the edge of the implanted area.

anisotropy of the milled structures is also a motivation of this work. We can make the etched profiles more anisotropic by truncating the bottom, more conical portions of the milled structures when wet etching to achieve suspended structures.

In order to investigate the etching rates and control the size of the suspended membrane, we applied different wet etching times and then obtained cross-sectional views by FIB milling again. In Fig. 5(a), we show the cross-sectional SEM image of a slab after 10 min of wet etching. The measured etching rate is ~100 nm/min, as shown in the inset with a larger magnification to demonstrate more details. There are tiny spots interspersed on the sample surface caused by material redeposition during milling. For conventional waveguides in LN fabricated by proton exchange, the propagation loss is high due to light leakage caused by poor refractive index contrast. Once the buried sacrificial layer is removed by the etchants, a symmetric cladding structure (air-LN-air) is formed, which can significantly enhance light confinement in the waveguide as well as reduce the propagation loss. To make a larger area of suspended slab, one can simply extend the wet etching time. The cross-sectional profiles of a slab and a post after 20 min of wet etching are shown in Figs. 5(b) and 4(c), respectively. The suspended slab is almost separated from the substrate by the etch. We noticed that the etching profile has a slightly tapered shape. This is because the outer part has been exposed to etchants for a longer time than the inner part, but it is also evident that this is not a serious problem and that the selectivity is generally quite uniform, even with long undercuts (which are not needed in PC-based structures).

We also fabricated suspended PCs in a LN slab, as shown in Fig. 6. The 13×12 hole array with a lattice constant of $a=800$ nm and a hole radius of $r=0.175a$ was milled by FIB for ~30 min using a small probe current. Taking into account both the spot size of milling holes with such small features and a reasonable total milling time, a 70 pA probe current (25 nm spot size) was selected. As we can see from the inset in Fig. 6, the holes have been milled through the suspended membrane. The structure is anisotropic because the bottoms of the milled cones have been truncated by the buried air layer. Since the thickness of the buried layer can be controlled by the ion implantation process, one can easily change the parameters of the fabricated suspended structures to tailor the device performance. The impact of a conical shape on PC slab waveguides was theoretically investigated by Tanaka *et al.*[19] and it was found that PC waveguides consisting of cone-shaped air holes exhibit a much larger propagation loss than in vertical air hole waveguides. They also explored that the coupling between TE-like waveguide modes and TM-like slab modes is responsible for the large propagation loss generated by cone-shaped PCs. Similar studies in annealed proton exchanged LN have also been performed by Burr *et al.*[20] recently. They experimentally verified that shallow conical holes could be used as a broadband attenuator. According to their results, only holes with nearly vertical (less than 0.5° tilting angle) sidewalls could produce well-defined stop bands in the transmission spectra.

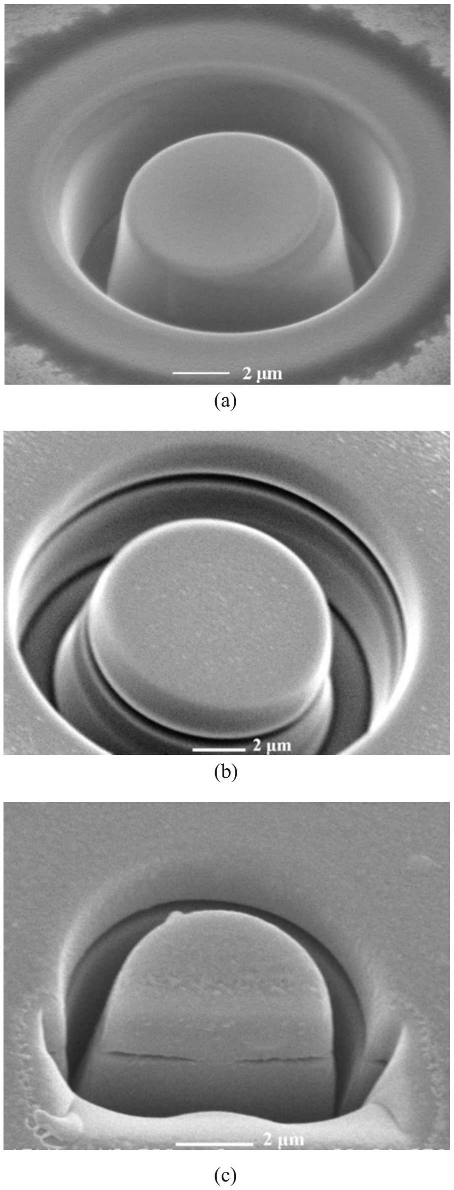

FIG. 4. (a) FIB image of a post after milling and before wet etching. (b) SEM image of a post after wet etching. (c) SEM image showing the cross-sectional view.

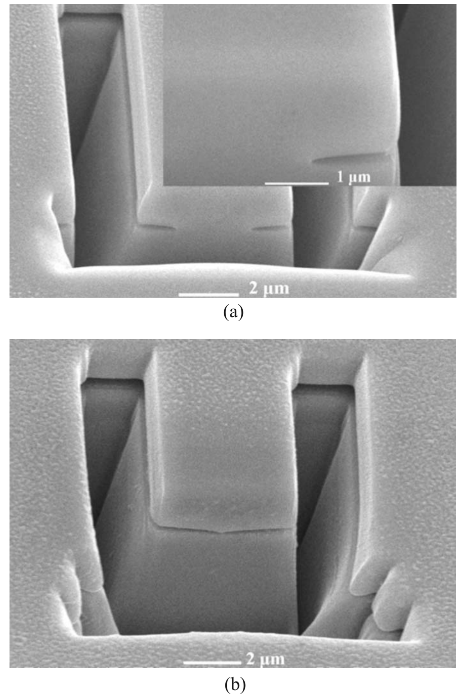

FIG. 5. Cross-sectional images showing the undercut after (a) 10 min and (b) 20 min of wet etching. The inset in (a) shows a further magnified view of the right undercut structure.

Thus, PC applications in LN require holes with vertical profiles to achieve an acceptable optical performance. Making the holes suspended can enable easy fabrication of vertical PCs because the bottoms of the tapered holes caused by redeposition during FIB milling would be truncated by an air gap. One can further minimize redeposition effects by coating a thin layer of metal before FIB milling and then wet etching to remove the metal together with redeposited material after FIB milling. In addition, we can also fabricate large area PCs with high aspect ratio by applying inductively coupled plasma etching on suspended LN membrane, which we plan to report after a thorough study. After truncating the bottoms of the cone-shaped holes, only the top parts with a uniform profile are left in the suspended membrane, which can further give rise to better performance. The ion implantation could also take place at multiple energies within the same sample, creating complicated layered structures of high-index contrast when undercut.

IV. CONCLUSION

In summary, we have investigated a novel method of fabricating suspended structures in LN including normal slab waveguides and PCs. After generating lattice damage with ion implantation, FIB milling was employed to make the buried sacrificial layer exposed to etchants during wet etch-

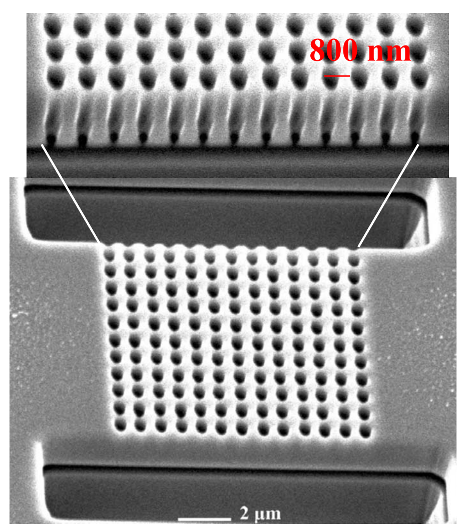

FIG. 6. (Color online) Fabricated PCs in a suspended slab. The holes have been milled through the slab.

ing. The measured etching rate is approximately 100 nm/min. The undercut structure has been demonstrated by a second FIB milling to show the cross-sectional profiles. Using this method, one can fabricate a suspended structure in LN without applying ion slicing and wafer bonding to transfer thin films, therefore avoiding thermal mismatch-induced stress during heating and cooling steps. In addition, our structure has a high-index contrast, which could lead to a strong light confinement and a low propagation loss simultaneously in the waveguide. Monolithic fabrication of large area PCs with high aspect ratio and uniform profiles is now realizable in LN.

ACKNOWLEDGMENT

The authors acknowledge funding from the National University of Singapore Cross-Faculty under Grant No. R263000529646.

[1]M.-P. Bernal, N. Courjal, J. Amet, M. Roussey, and C. H. Hou, Opt. Commun. **265**, 180 (2006).
[2]M. Roussey, M.-P. Bernal, N. Courjal, D. Van Labeke, F. I. Baida, and R. Salut, Appl. Phys. Lett. **89**, 241110 (2006).
[3]M. Roussey, M.-P. Bernal, N. Courjal, and F. I. Baida, Appl. Phys. Lett. **87**, 241101 (2005).
[4]T.-J. Wang, C.-F. Huang, W.-S. Wang, and P.-K. Wei, J. Lightwave Technol. **22**, 1764 (2004).
[5]T.-L. Ting, L.-Y. Chen, and W.-S. Wang, IEEE Photonics Technol. Lett. **18**, 568 (2006).
[6]H. Hu, A. P. Milenin, R. B. Wehrspohn, H. Hermann, and W. Sohler, J. Vac. Sci. Technol. A **24**, 1012 (2006).
[7]Z. Ren, P. J. Heard, J. M. Marshall, P. A. Thomas, and S. Yu, J. Appl. Phys. **103**, 034109 (2008).
[8]Y. A. Vlasov, M. O'Boyle, H. F. Hamann, and S. J. McNab, Nature (London) **438**, 65 (2005).
[9]S. J. McNab, N. Moll, and Y. A. Vlasov, Opt. Express **11**, 2927 (2003).
[10]E. Dulkeith, S. J. McNab, and Y. A. Vlasov, Phys. Rev. B **72**, 115102 (2005).
[11]Y.-B. Park, B. Min, K. J. Vahala, and H. A. Atwater, Adv. Mater. (Weinheim, Ger.) **18**, 1533 (2006).
[12]M. Levy, R. M. Osgood, Jr., R. Liu, L. E. Cross, G. S. Cargill III, A. Kumar, and H. Bakhru, Appl. Phys. Lett. **73**, 2293 (1998).
[13]D. Djukic, R. M. Roth, R. M. Osgood, Jr., K. Evans-Lutterodt, H. Bakhru, S. Bakhru, and D. Welch, Appl. Phys. Lett. **91**, 112908 (2007).
[14]P. Rabiei and P. Gunter, Appl. Phys. Lett. **85**, 4603 (2004).
[15]P. Rabiei and W. H. Steier, Appl. Phys. Lett. **86**, 161115 (2005).
[16]F. Schrempel, T. Gischkat, H. Hartung, T. Höche, E.-B. Kley, A. Tünnermann, and W. Wesch, Opt. Lett. **34**, 1426 (2009).
[17]F. Sulser, G. Poberaj, M. Koechlin, and P. Günter, Opt. Express **17**, 20291 (2009).
[18]See http://www.srim.org/.
[19]Y. Tanaka, T. Asano, Y. Akahane, B.-S. Song, and S. Noda, Appl. Phys. Lett. **82**, 1661 (2003).
[20]G. W. Burr, S. Diziain, and M.-P. Bernal, Opt. Express **16**, 6302 (2008).